PROCEEDINGS OF SPIE

SPIEDigitalLibrary.org/conference-proceedings-of-spie

MSE acquisition and guider system focal plane hardware conceptual design

Gillingham, Peter, Salmon, Derrick, Flagey, Nicolas, Szeto, Kei, Murowinski, Richard, et al.

Peter R. Gillingham, Derrick Salmon, Nicolas Flagey, Kei Szeto, Richard Murowinski, Will Saunders, "MSE acquisition and guider system focal plane hardware conceptual design," Proc. SPIE 11445, Ground-based and Airborne Telescopes VIII, 1144548 (13 December 2020); doi: 10.1117/12.2561086

SPIE.

Event: SPIE Astronomical Telescopes + Instrumentation, 2020, Online Only

Downloaded From: https://www.spiedigitallibrary.org/conference-proceedings-of-spie on 26 Jan 2021 Terms of Use: https://www.spiedigitallibrary.org/terms-of-use

MSE Acquisition and Guider System Focal Plane Hardware Conceptual Design

Peter Gillingham[a], Derrick Salmon[b],Nicolas Flagey[b], Kei Szeto[b],
Richard Murowinski[b], Will Saunders[a]

[a]Australian Astronomical Optics- Macquarie University, 105 Delhi Road, North Ryde NSW 2113, Australia;
[b]Canada France Hawaii Telescope, 65-1238 Mamalahoa Highway, Kamuela, HI 96743 USA

ABSTRACT

We discuss the Maunakea Spectroscopic Explorer (MSE) Acquisition and Guide (A&G) System conceptual focal plane hardware and operational requirements and pay detailed attention to the A&G system's three CMOS cameras' areas and sensitivities needed to assure a high success rate in acquiring suitable guide stars. Ways to provide auxiliary functions, including the measurement of defocus and misalignment of the telescope optics, are also discussed.

Keywords: MSE, multi object spectrograph, acquisition and guiding, A&G, star counts

1. INTRODUCTION

With the advent of several large telescopes soon to be commissioned or already online producing deep all-sky imaging surveys a natural follow on capability is a wide field deep spectroscopic survey. The Maunakea Spectroscopic Explorer (MSE) is a spectroscopic survey telescope intended to replace the 3.6 m CFHT telescope on Maunakea, Hawaii.[1] MSE's 11.25 m diameter multi-segment primary mirror and its prime focus wide field corrector[2] will feed an hexagonal array of 4332 100 μm fibers[3] feeding multiple medium and high resolution spectrographs mounted on the telescope structure or located remotely in the telescope building. The fast f/1.9 focal surface and its 1.6º field with an image scale of 105 μm per arcsec present unique challenges for field acquisition and guiding. Here, we take account of the MSE requirements for the operational performance of the Acquisition and Guiding system, paying detailed attention to the sensors' areas and sensitivities needed to assure a high success rate in acquiring suitable guide stars. Ways to provide auxiliary functions, including the measurement of defocus and misalignment of the telescope optics, are also discussed and specified.

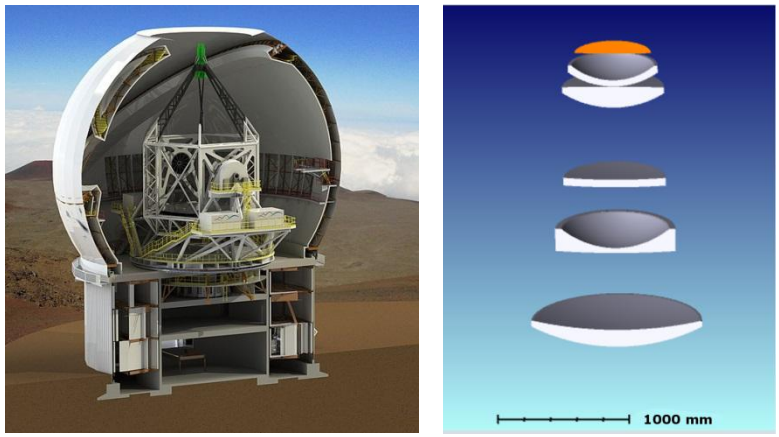

Figure 1. The MSE telescope and enclosure (left) and a cross section view of the prime focus corrector (right) with the focal surface shown in orange.

Ground-based and Airborne Telescopes VIII, edited by Heather K. Marshall, Jason Spyromilio, Tomonori Usuda, Proc. of SPIE Vol. 11445, 1144548 · © 2020 SPIE
CCC code: 0277-786X/20/$21 · doi: 10.1117/12.2561086

Downloaded From: https://www.spiedigitallibrary.org/conference-proceedings-of-spie on 26 Jan 2021
Terms of Use: https://www.spiedigitallibrary.org/terms-of-use

The MSE acquisition and guiding (A&G) system considered here uses three CMOS detectors located at the telescope focal surface beside the fiber positioners. The system's primary functions are field acquisition, the rapid identification and selection of suitable guide stars and the feeding of telescope and field rotator tracking signals to the telescope control system. The A&G cameras must incorporate fiducial position markers to tie the camera pixel arrays to the fiber metrology system's coordinates. To maintain observing efficiency, the system must work for at least 95% of directions randomly selected over the sky accessible to MSE.

The key A&G system requirements include:

1. The use of three cameras positioned on alternate sides of the hexagonal science field.
2. There is a very strong preference for avoiding any vignetting of the science field due to the feeds to these cameras.
3. With 1 exposure per second on 1 guide star in each camera, centroid errors are to be no greater than 7 μm rms 1-D (i.e. ~ 0.07arcsec) and this should apply with the 90th percentile delivered image quality, i.e. the value that is exceeded only in 10% of cases, estimated to have a FWHM of 0.79 arcsec at 500 nm.
4. The sensor areas are to be large enough for finding guide stars in all three cameras to satisfy requirement #3 over at least 95% of the sky available to MSE.
5. The system should provide for the measurement of any de-focus or misalignment of the telescope optics sufficient to cause any significant fall in energy injected into the optical fibers.
6. Fiducial sources for which positions can be measured by the fiber metrology system are to be provided with each camera. Their positions with respect to the camera sensor area should be stable to within 1μm.

An additional practical requirement is that the cameras be fixed rigidly in position with respect to the fiber array without lateral or focus motion control. This arises due to the limited space available for mounting the A&G cameras, for the sake of system simplicity and due to the need for camera positioning stability. However, since the A&G camera will be mounted to the field rotator assembly, the cameras will have the freedom to explore potential A&G fields using the field rotator inherent in the design of any alt-az telescope

2. A&G CAMERA PLACEMENT

We have elected to locate the three A&G cameras directly on the MSE focal surface on alternate edges of the hexagonal fiber array which patrol the science field. This avoids vignetting using diagonal feeds to the cameras, as suggested in figure 2.

Downloaded From: https://www.spiedigitallibrary.org/conference-proceedings-of-spie on 26 Jan 2021
Terms of Use: https://www.spiedigitallibrary.org/terms-of-use

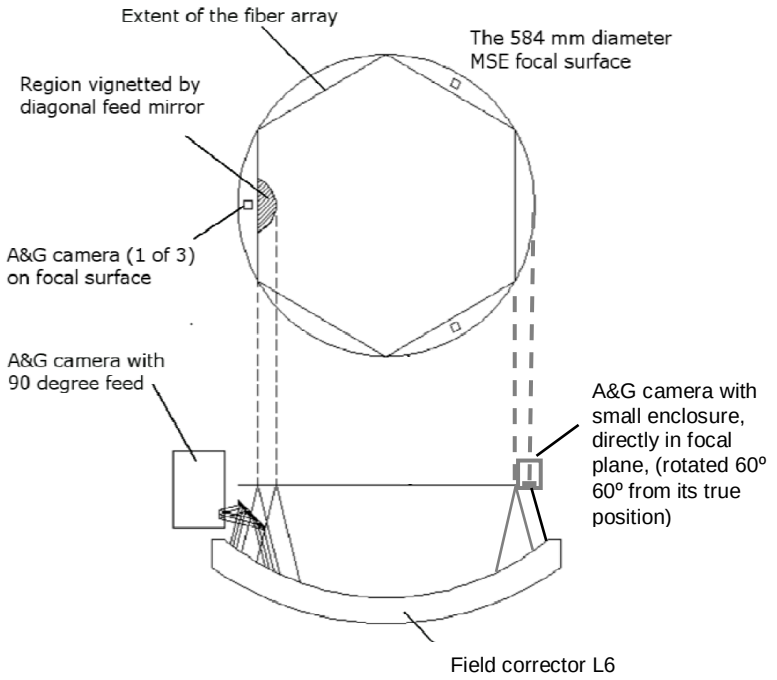

Figure 2. A schematic representation of the MSE focal surface geometry. The area covered by the hexagonal fiber array and the last lens of the wide field corrector are shown. The arrangement that was first considered, with guide cameras fed through mirrors, is compared with the current intention, using very compact cameras, to mount them directly in the focal surface, avoiding any vignetting.

3. STELLAR MAGNITUDE THRESHOLD NEEDED FOR FIELDS WITH FEW STARS

The aim to mount the three cameras without vignetting any of the science field was a strong driver to minimize the size of each camera enclosure, which suggested that the sensor area should be no bigger than necessary. So considerable effort was put into determining this minimum. We looked in detail (reference 4) at the success rate with a particular detector area and a range of stellar magnitudes near the North galactic pole. We concluded from simulations with 1000 pointings at random offsets of up to 1º from the galactic pole that, for fixed locations in the MSE field of three sensors each having an area of 1.22 cm^2 (that of a very compact off-the-shelf camera that had been identified as a possible choice) sufficient sensitivity to work with an i magnitude of 21 would give a success rate of 96% while magnitudes 20 and 19 would give success rates of 80% and 40% respectively. Considering that the requirement is for achieving suitable centroiding accuracy over 95% of the whole sky available to MSE, these success rates within 1º of the galactic pole indicate that sufficient sensitivity to work with 20th magnitude stars would surely be adequate and a 19th magnitude threshold would probably suffice.

Furthermore, there would generally be the option, in planning the observing setup, of changing the position angle of the observation. So, even very close to the galactic pole, with a threshold of 19th magnitude giving a failure rate of ~60% for a fixed position angle, the freedom to choose the position angle over a range of several degrees would reduce this failure rate to < 5%. In the event that such tuning of the position angle was undesirable, through requiring neat tiling of adjacent hexagonal fields, a choice of six position angles could be provided by having the three sensor areas depart from equal angular spacing, e.g. having their relative position angles 0, 118º, and 242º. Then six distinct sets of sensor areas would be available while retaining neat tiling of the hexagonal fields.

Rotating the detector assembly through an integer x 60º in addition to whatever change in position angle is required with the new telescope attitude might delay the setting on a new field but it should be needed on only a very small fraction of settings since failure to find three suitable guide stars on the initial position angle should be rare, even near the galactic pole. So, a sensitivity that would give the required centroiding accuracy with an i magnitude of 19 would comfortably meet the requirement with sensor areas each ~1.2 cm^2.

Downloaded From: https://www.spiedigitallibrary.org/conference-proceedings-of-spie on 26 Jan 2021
Terms of Use: https://www.spiedigitallibrary.org/terms-of-use

4. STELLAR MAGNITUDE THRESHOLD NEEDED FOR CROWDED FIELDS

In reference 5 we examined the availability of stars of suitable magnitudes sufficiently separated from neighbours to serve as good guide stars in the vicinity of the galactic centre.

Looking at all stars within each of the three fields of i magnitude 20 and brighter, the brightest was checked and discarded if there were any neighbours within a square 10 arcsec on a side centred on the candidate star. If it was discarded, the test was applied to the next brightest and so on. In all 1000 trials with the telescope pointing randomly within a radius of 0.5º of the centre for the test (at Galactic longitude 50º and latitude +1º) a suitable guide star of magnitude 17 or brighter passed this selection test in all three guider fields. There were, on average, about 75 stars in each field; in the vast majority of cases, the successful star was the brightest in the field; in the worst case across the three cameras and 1000 pointings, it was the 5th brightest.

This trial indicated that a camera with sensor area 1.22 cm^2 need only guide satisfactorily on a star of 17th magnitude to easily meet the requirement at the galactic centre.

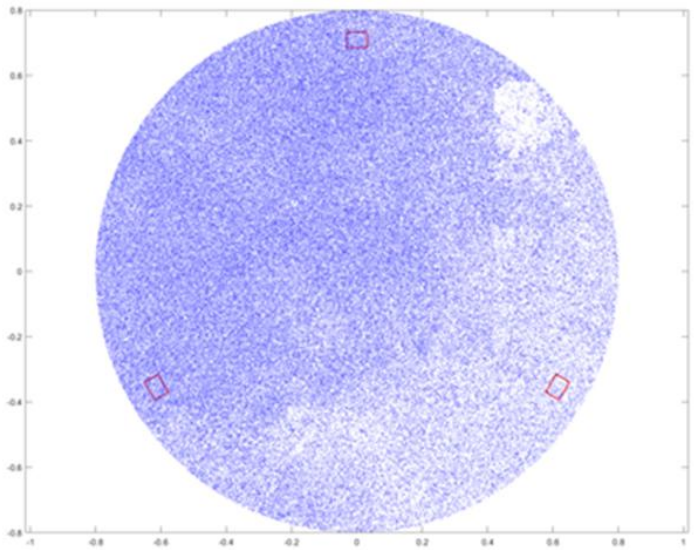

Figure 3. the 1.52° MSE field pointed at the centre of the selected SDSS star field with stars of magnitude 21 and brighter

Downloaded From: https://www.spiedigitallibrary.org/conference-proceedings-of-spie on 26 Jan 2021
Terms of Use: https://www.spiedigitallibrary.org/terms-of-use

5. MAGNITUDE THRESHOLD SET BY SENSOR PROPERTIES

In reference 6 we calculated the rms centroid error as a function of stellar magnitude with the CMOS detector, the near Infrared version of the On-Semi Python 5000 sensor, as fitted to the Teledyne DALSA M2590-NIR camera (reference 7), with the quantum efficiency shown in figure 4. For optimum discrimination against the sky, the camera would be filtered to exclude radiation below ~ 650 nm.

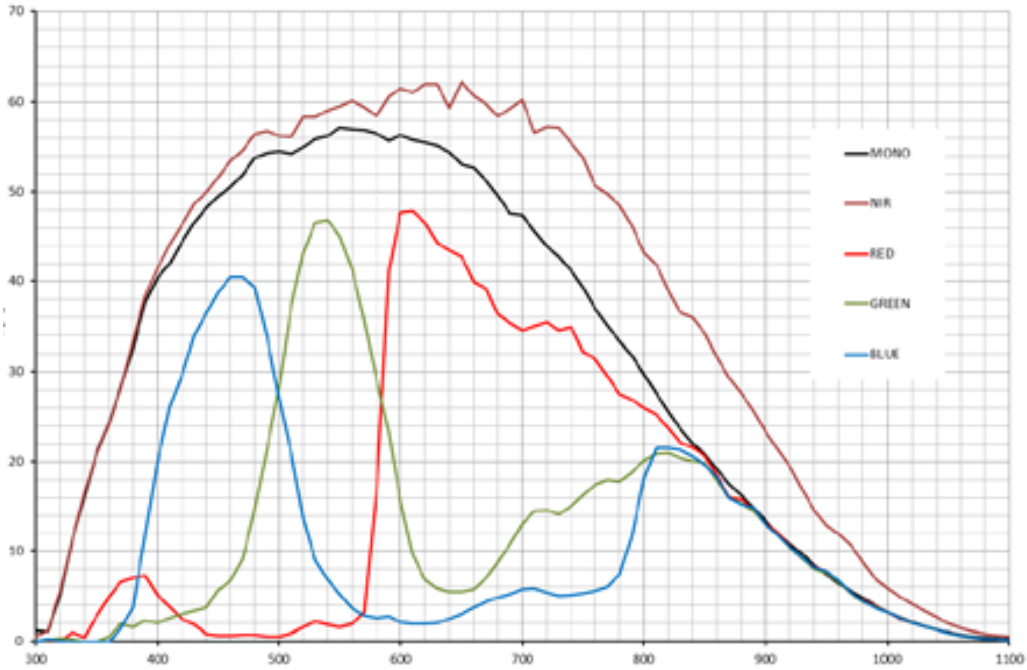

Figure 4. Quantum efficiencies for On-Semi Python 5000 sensors. The NIR values in the uppermost curve are applicable

The image quality at the MSE field periphery (at radius 0.76º) was checked for the MSE optics design with combined wavelengths 700, 800, and 900 nm with weights 3, 2, and 1 respectively. The weighted rms radius given by ray-tracing was just under 0.12 arcsec.

Table 1 shows the parameters used as input to the sensitivity calculation. As noted earlier, the image FWHM adopted was equivalent to 0.79 arcsec. “Pixsize” was the side of a 3 x 3 bin of sensor pixels each 4.8 μm square. Note that the exposure time “Etime” was set to 1 second.

Downloaded From: https://www.spiedigitallibrary.org/conference-proceedings-of-spie on 26 Jan 2021
Terms of Use: https://www.spiedigitallibrary.org/terms-of-use

Table 1. Input parameters for On-Semi Python 5000 NIR CMOS sensor

Fwhm (mm)	0.0864
Pixsize (mm)	0.0144
Arraysize (pixels)	18
RandAmp (pixels)	1.0
Mag	range entered at input
Lam (nm)	825
Dlam (nm)	350
A (m^2)	80
QE	0.38
Readnoise (e-)	30.0
Darknoise (e-)	4.0 * Etime
Etime (sec)	1.0
Msky	19
Pix (arcsec)	0.133
Zd (degrees)	30
ExtCoeff (mag/airmass)	0.1
RPm	0.90
Topt	0.90
Numpix (pixels)	5
c1,c2,c3	0,0,0
Thresh	2.0

The calculation of centroiding error included allowances for stellar photon noise and additive Poisson noise due to sky background, dark noise, and detector read noise, with the specified seeing FWHM of 0.79 arcsec. Figure 5 indicates that the required rms error of 7 µm could be reached with a stellar magnitude as faint as ~21.

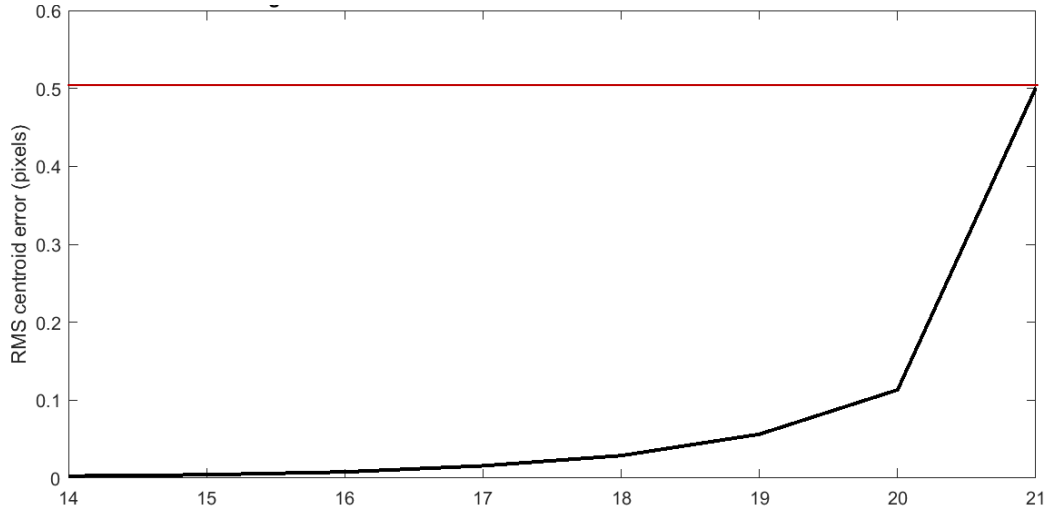

Figure 5. rms centroid error (pixels, each 14.4 µm on a side) vs AB magnitude 650 to 1000 nm. The red line is at the required rms accuracy of 7 µm or ~ 0.49 x Pixsize.

Downloaded From: https://www.spiedigitallibrary.org/conference-proceedings-of-spie on 26 Jan 2021
Terms of Use: https://www.spiedigitallibrary.org/terms-of-use

6. COMBINING SIMULATIONS OF STAR DISTRIBUTIONS AND CAMERA SENSITIVITY

The star distribution calculations indicated that stars as bright as 19th magnitude should be found reliably in all three guide fields, each with an area of ~ 1.22 cm^2 while the calculation of the sensor performance indicates that a 21st magnitude star would just suffice to give the required centroiding accuracy. So the conclusion is that there will be a useful safety margin in adopting an off the shelf compact camera with 1.22 cm^2or greater sensor area. If operation with more exposures/second or with a more restricted wavelength range was deemed desirable, there would be some scope for such a change.

7. SPACE FOR FITTING CAMERAS

The optical design field of MSE is 583.2 mm in diameter and the hexagon inscribed within that circle is 505.1 mm across flats. We assume that the array of positioner spines at their home positions will fill this hexagon and that spines can tilt radially outward so their tips are up to10 mm from their home positions. Then the distance from the outermost spine tips to the outer perimeter of the optical field is (583.2 – 505.1)/2 – 10 mm = 29.05 mm. So the distance ***d*** from the side of a camera enclosure to the far side of its sensor should not exceed 29 mm if it is to clear the spine tips and to have all its sensitive area within the optical field.

In the case of the camera considered in Section 5 in relation to its sensor area and sensitivity, ***d*** is 19.4 mm, well inside the limit.

8. CANDIDATE CAMERAS/SENSORS

By the time cameras must be purchased for MSE, the options will be different than they are at present, and presumably better. However, examining specifications of those currently available is necessary to confirm the feasibility of the proposed system. And it will be wise to buy a camera soon to allow for full assessment of the suitability of such devices.

A range of digital cameras from Teledyne DALSA, Canada (reference 7) includes several with small enclosures and acceptable sensor areas. The most suitable initially appeared to be the model Genie TS-M2560 with 2560 x 2048 pixels 5 µm square (i.e. with an area 1.31 sq cm) and an envelope 49 x 49 x 54 mm. This model was adopted in making the CAD model illustrated in figure 6. Later it was found that another DALSA camera would be better suited but its mounting to the Sphinx fiber positioner could be virtually the same. Its dimensions are indicated in figure 7.

The recommended choice is M2590-NIR with an On-Semi Python 5000 sensor having 2592 x 2048 pixels 4.8 µm square, giving an area of 1.223 cm^2. Its advantage would be the option of a "near infrared" sensor having peak quantum efficiency at 650 nm of 61% (as in figure 4) and, probably, a lower dark noise. The on-line data-sheet for this sensor is rare in quoting the dark noise. This is listed as 9.3e^-/second at 20ºC, halving with a 5.2º reduction in temperature. Considering that a 1 second exposure time is likely to be the longest that is appropriate and that the ambient temperature should generally be < 5ºC, the noise performance of such a sensor should be completely satisfactory without cooling below ambient.

Binning of pixels and limiting readout to specific small regions of interest are available as standard in these cameras. Their power dissipations are given as up to 5W for each camera.

Downloaded From: https://www.spiedigitallibrary.org/conference-proceedings-of-spie on 26 Jan 2021
Terms of Use: https://www.spiedigitallibrary.org/terms-of-use

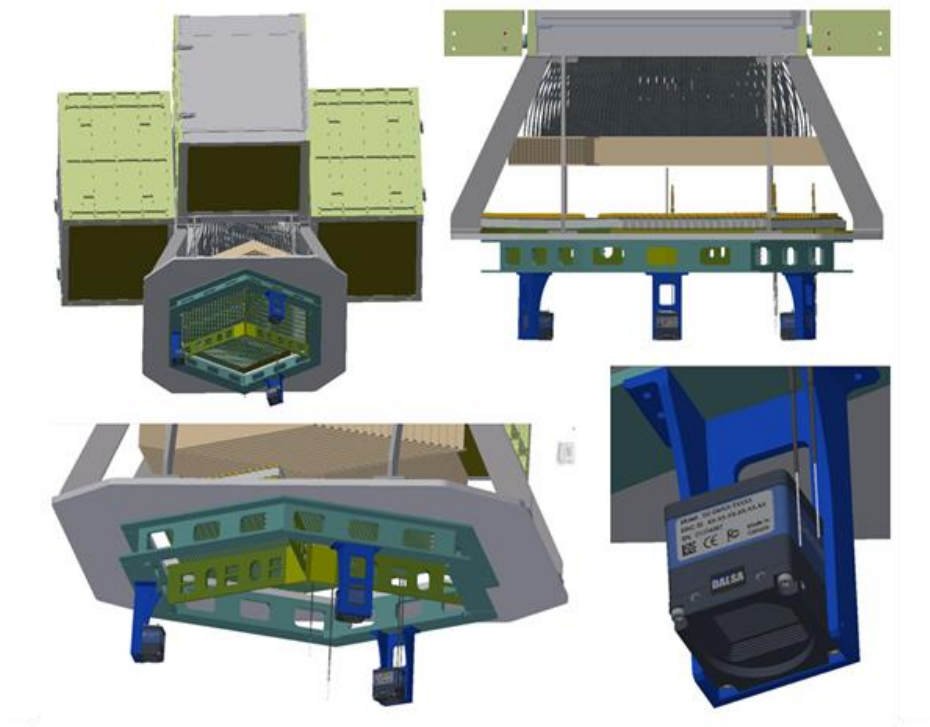

Figure 6. CAD model of three cameras mounted on the Sphinx fiber positioner. Only a few of the positioner spines are shown.

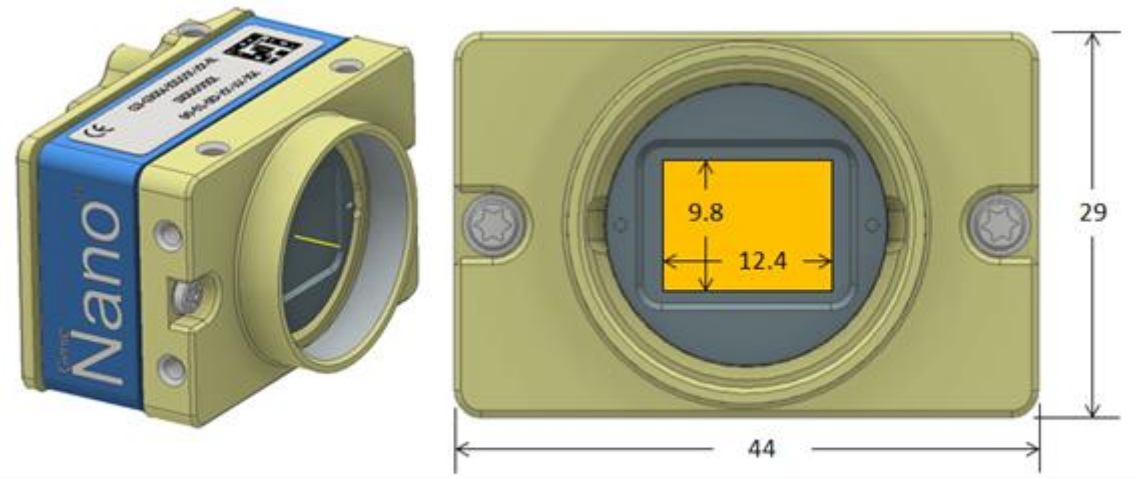

Figure 7. Genie Nano camera M2590-NIR. Dimensions: mm. The dimension *d*, defined in Section 7, is 29/2 + 9.8/2 = 19.4 mm.

Downloaded From: https://www.spiedigitallibrary.org/conference-proceedings-of-spie on 26 Jan 2021
Terms of Use: https://www.spiedigitallibrary.org/terms-of-use

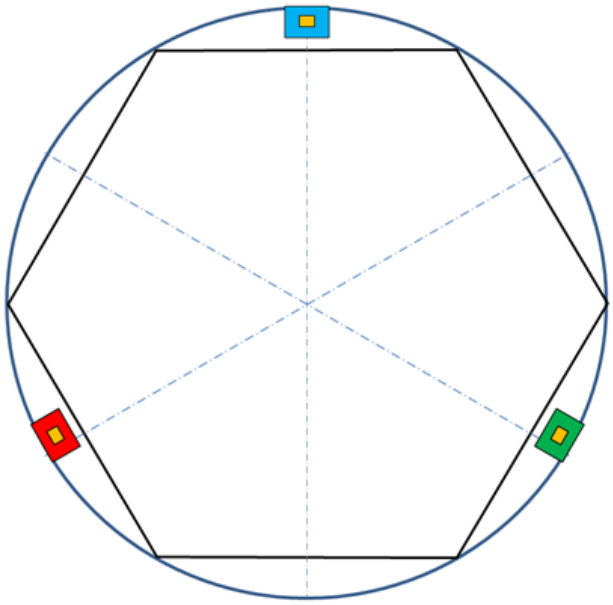

Figure 8. Camera positions in relation to circular optical field and hexagonal science field, offset from equal angular spacing

9. MICRO-LENS ARRAYS ON SENSORS

The sensors have arrays of micro-lenses with one over each pixel. With the focal ratio on MSE ~ f/1.9, some light passing through the lens does not reach the photo-diode. With data given on the On-Semi web site for the Python 5000 sensor, a calculation (reference 8) indicates a loss of ~ 7% at the centre of the sensor area. There could be concern about whether this lost light might find its way to the wrong diode and degrade resolution, but any such effect will be lessened by the intention that the sensor will always be used with bins of at least 3 x 3 pixels.

There is some further loss because the micro-lens pitch is made a little less than the pixel pitch so that there is a small radial offset between the micro-lens axis and a diode centre at the outside of the field. This increases the collection of light onto these outer pixels with a lens exit pupil ~ 80 mm from the sensor, as in typical industrial applications. With our pupil many meters from the sensor, however, this results in a further loss of sensitivity, calculated as reaching ~ 2% at the corners of the small sensor under consideration.

10. MEASUREMENT OF DEFOCUS, WFC MISALIGNMENT, AND FLAT FIELD CALIBRATION

10.1 Minimal Plan

It was initially expected that provision would be needed for re-setting the axial positions of the guide cameras so as to explore over a range of focus in the process of checking for and correcting temporal changes in the telescope focus. In a note “MSE control of focus”(reference 9), it is argued that with appropriate calibration of the telescope’s flexure and allowance for steelwork temperatures measured at several relevant points, an optical check for defocus each time the telescope is set on a new field should easily suffice for maintaining good focus. (On both the CFHT and the AAT such a check is warranted at most only once/night.)

Downloaded From: https://www.spiedigitallibrary.org/conference-proceedings-of-spie on 26 Jan 2021
Terms of Use: https://www.spiedigitallibrary.org/terms-of-use

In a note "MSE – detecting top end misalignment from out of focus images" (reference 10) it was shown that analysis of images taken with focus settings at ± 0.4 mm from best focus suffice to measure both defocus and corrector misalignment to adequate accuracy to avoid significant loss of injection efficiency into the smaller fibre cores (as suited to the higher resolution spectrographs).

Combining the conclusions from these two notes, it should be adequate to record the out-of-focus images only in between science exposures and achieve the required de-focus settings with the hexapod that supports the telescope top end. So the minimal plan was to provide no mechanisms external to the cameras. However, it is apparent that a wheel with windows of differing thicknesses just ahead of each camera to give the focus offsets, would be very useful

10.2 A filter/shutter wheel for each camera

It should be possible to provide a wheel with, say, 6 optional positions, for each camera, as suggested in figure 9, without any vignetting of the science field. The wheel could house three filters identical in spectral transmission but having different optical thicknesses to provide for making the defocused tests more quickly and probably with greater accuracy in the amount of defocus than employing the hexapod. In one additional position there could be a shutter to be used in conjunction with light sources for flat field calibrations.

11. EMPLOYING AN OPTIONAL HIGHER EXPOSURE RATE FOR TIP/TILT CORRECTION

A specification of 10 exposures/second adopted in 2018 was changed in 2019 to one/second. But the calculations of stellar distributions and sensor sensitivity have indicated that the faster rate could be achieved with the compact off-the-shelf cameras. Such a fast rate would be un-necessarily high if correction of the angular error was dependent entirely on the azimuth and elevation drives. There is also some doubt whether seeing-driven image motion will be sufficiently coherent across the full field to make correction with a bandwidth as high as a few Hz worthwhile. And from experience on Keck, with its exposure of a larger top end to wind through a much larger dome opening, wind-driven oscillation with MSE should seldom need correction. However, if it is concluded that such correction is really beneficial, then an option will be to drive one element of the wide field corrector lens. Ray-tracing has confirmed that image displacements 1 arcsec peak to peak could be applied in this way with no significant change in aberrations.

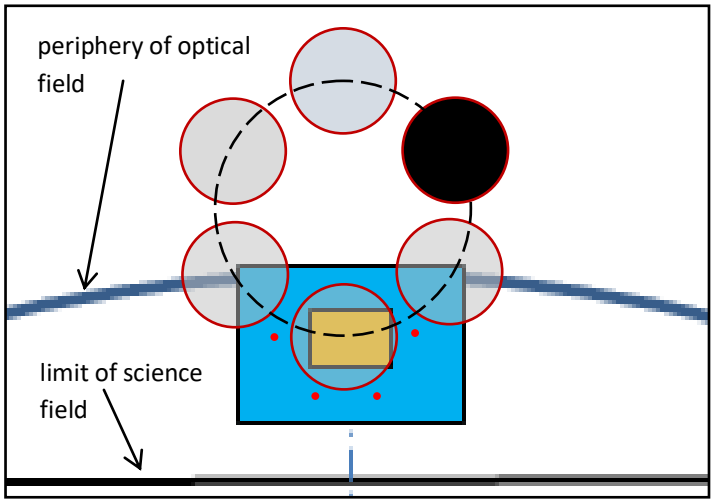

Figure 9. Approximate layout for filter wheel ahead of camera. The height of the segment between the optical field periphery and the science field limit is 39mm. The red dots suggest where LEDs could be mounted on the camera

Downloaded From: https://www.spiedigitallibrary.org/conference-proceedings-of-spie on 26 Jan 2021
Terms of Use: https://www.spiedigitallibrary.org/terms-of-use

12. OPTION OF MORE SUITABLE CAMERAS

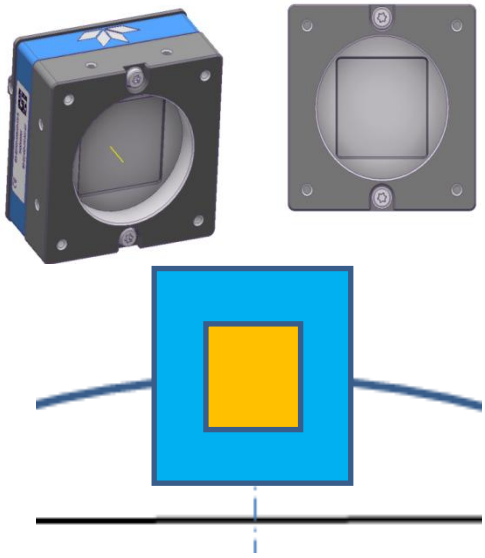

Figure 10 Views of Genie Nano XL M 5100 camera and how it would relate to the margins of the scientific and optical fields. Its enclosure is 59 x 59 mm and the sensor surface is 23 mm square, so ***d*** = 41 mm .

Figure 11. Camera with Sony IMX 387 sensor
d ≈ (32+10.6)/2 ≈ 21mm
Sensor 18.9 x 10.6mm, area 2.0 sq cm

While the calculations discussed above indicate that sensors with areas as small as ~1.2 cm^2 should be adequate, it is likely cameras with larger sensor formats can be accommodated to advantage. Figure 10 shows views of the larger Genie Nano XL M5100 NIR camera with a sensor area of 5.3 cm2, indicating that it would exceed the d <29mm criterion suggested in Section 7 so not all its sensitive area would lie within the optical field.

However, the range of cameras available is bound to increase and a better option than the DALSA M2590-NIR is very likely to be available by the time the camera choice must be finalized.

Figure 11 shows a camera that looks close to being ideal, although only a few details are available so far. It uses the Sony IMX 387 CMOS sensor which has a favourable aspect ratio (1.77:1) giving 2.0 cm^2 area with ***d*** only 21 mm. However, it is not listed as having a NIR version.

A larger pixel size than the 4.8 x 4.8 µm of the M2590 would also be advantageous since such small pixels would always be binned at least 3 x 3 to suit the ~ 105 µm/arcsec scale of MSE. With larger pixels it is likely that the inefficiency in the action of the micro-lens array would be reduced

Downloaded From: https://www.spiedigitallibrary.org/conference-proceedings-of-spie on 26 Jan 2021
Terms of Use: https://www.spiedigitallibrary.org/terms-of-use

13. FIDUCIALS FOR LOCATION OF THE GUIDING FIELDS

13.1 Stability needed in fiducial positions

The metrology system for controlling the positioning of fibres will need to accurately establish the relationship between the X/Y coordinates of the guiding cameras and the positioner. Simply mounting a few very small surface mount LEDs on the front face of each camera enclosure should provide suitable fiducials. In the case of the M2590-NIR camera, this face is only ~ 1.2 mm ahead of the sensor surface. With the extremely slow focal ratio of the metrology optics (~ f/150 at the MSE focus), the slight departure from parfocality of these fiducials with respect to the sensor will be completely harmless.

The tolerance on stability of these fiducials with respect to the sensor coordinates was specified in reference 1 as 1 µm. This is unnecessarily tight considering that the change due to differential atmospheric refraction in relative positions of star images at the centre of the telescope field and its periphery during a science exposure will often be ~ 10 times greater. Figure 12 shows the result of ray-tracing the MSE optics to quantify the drift due to differential refraction. The MSE corrector design includes, as a feature of its ADC, provision for reducing this drift. Without this feature, the drift would be roughly 2 times greater. To quantify the relative drift requires that the refraction be simulated in a more rigorous way than Zemax provides. (The standard "atmospheric" surface in Zemax applies the same angular offset across the whole field.)

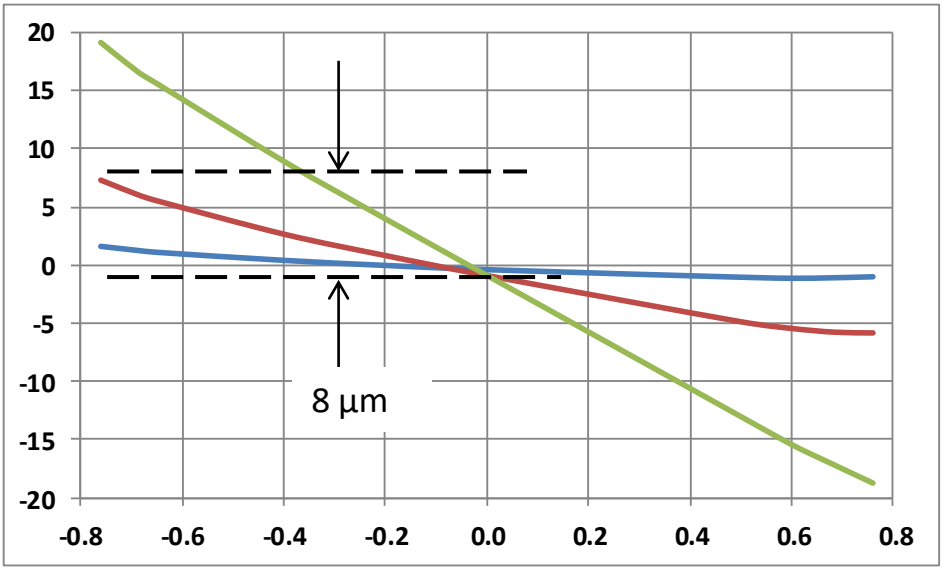

Figure 12. Relative image drift due to atmospheric refraction. Change in a star's image position (µm) due to atmospheric refraction with changing ZD along the 1.52º vertical diameter of the MSE field with a 5º change in ZD (which can be exceeded during a science exposure). The blue curve shows the differential drift for ZD changing between 0 and 30º, the red between 30º and 50º, and the green between 50º and 60º. So for a ZD around 40º, the separation between a star image on an auto-guider could change relative to an image at the field centre by ~ 8 µm during a science exposure of ~ 30 minutes (and twice that relative to a star at the far side of the field.

Downloaded From: https://www.spiedigitallibrary.org/conference-proceedings-of-spie on 26 Jan 2021
Terms of Use: https://www.spiedigitallibrary.org/terms-of-use

13.2 Effect of fiducials' wavelength on measurement of their positions

The metrology camera views the camera fiducials through the wide field corrector so the apparent positions of the fiducials depend on the setting of the ADC. Figure 13 indicates the magnitude of this effect with the ADC set for ZD 60º. At 650 nm, the slope of the curve is equal to:

1.141 -2 x 0.0006687 x 650 µm/nm = 0.272 µm/nm

So it would be desirable to know the effective wavelength of the LED emission at the time of the measurement to within ~ 3 nm so the wavelength uncertainty would never contribute an error more than 1 µm. With the requirement to switch on the LEDs a very short time before the metrology exposure, knowledge of how their spectral emission changes as they heat up will be needed. At ZD 30º, the dependence would be 3 times less and at ZD 45º, √3 times less.

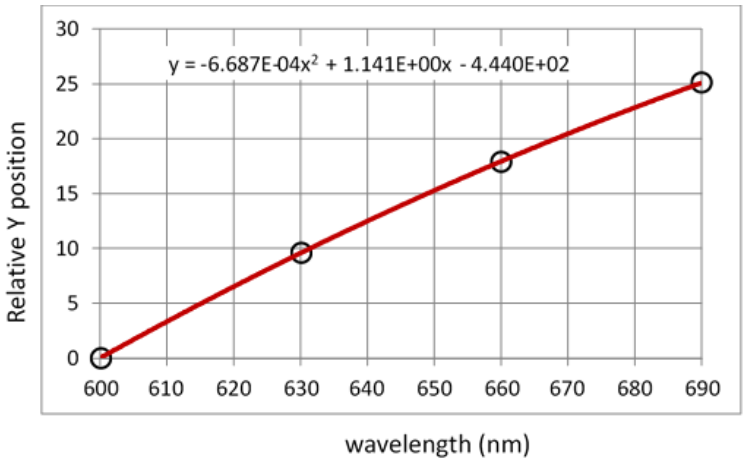

Figure 13 Dependence on wavelength of apparent position of a fiducial observed through the MSE ADC set for ZD 60º

14. EFFECTS OF GUIDE CAMERA POWER DISSIPATION

14.1 Significance of camera power dissipations

Between the three cameras, the heat dissipation with the cameras examined here would be up to 15W. This exceeds the maximum in the draft requirements document (reference 1) of 5W. However, air temperature inhomogeneity next to the cameras, so close to the focal surface, is less harmful than it could be elsewhere, e.g. in the beam approaching the primary mirror, where the large distance to the focus leads to much greater displacement of rays at the image for a given air temperature gradient. So the relevant criterion for permissible heat dissipation to the air is most appropriately how much is added to the overall heat convected from the top end. With the telescope at the zenith, the enclosures for Sphinx electronics have vertical surfaces with a total area > 4 m^2. For these enclosures cooled so their external surfaces have a temperature excess of 1ºC over the ambient air the heat convected from these surfaces will still be at least 90W. Sources associated with the rotation drive and the top end hexapod are likely to add significantly to this. So a 15W contribution from the cameras will have only a minor additive effect.

14.2 An estimate of seeing degradation due to top-end heat dissipation

In order to quantify seeing degradation due to heat dissipation at a top end, Beckers et al (reference 11) performed a series of measurements of image profiles with heat sources on the top end vanes of an ESO 2.2-m telescope. They observed that the effect on image quality was predominantly to reduce the intensity in the image core through spreading light widely, rather than increasing the FWHM. The relationship derived from these experiments led to their conclusion that, for an 8-m diameter telescope, heat dissipation of even 500 W would decrease the energy in the image core by only

Downloaded From: https://www.spiedigitallibrary.org/conference-proceedings-of-spie on 26 Jan 2021
Terms of Use: https://www.spiedigitallibrary.org/terms-of-use

~ 1%. So it is expected that the MSE observing efficiency will not be significantly degraded by the top end heat dissipation and that any additional loss due to the guide cameras will be negligible.

15. NO NEED FOR COOLING OR TEMPERATURE CONTROL OF CAMERAS

In the calculations of the signal to noise ratio of the camera to determine its accuracy in measuring an image centroid, the dark noise of the sensor and its change with temperature was taken into account assuming an ambient temperature of 5.1^{o}C (1^{o}C above the air temperature exceeded during Megacam exposures on the CFHT only 10% of the time). So it is clear that no cooling is needed to lower the dark noise. From the discussion above, it is also concluded that there is no need to have coolant flow to extract the few watts dissipated by each camera from the point of view of local seeing. Thus, it is safe to plan no cooling or temperature control of the cameras, simplifying their installation and avoiding adding to the hazard posed by coolant leaks.

16. SUMMARY

1. Careful calculations of the sensor area needed for very reliable acquisition of three suitable guide stars over the accessible sky have indicated that an area of ~ 1.2 sq cm will suffice with the sensitivity of visible/near infrared CMOS detectors currently available.
2. For such small sensors, there may very occasionally be a need for a special choice of position angle for an observation to find suitable guide stars on all three cameras. But the associated time lost should be negligible.
3. By the time the choice of cameras must be finalised, some that are more suitable should be available, being sufficiently compact to suit the space restrictions but with larger sensor areas.
4. The purchase of a camera of the class being considered in the near future (without waiting for the ideal model) will allow tests to be conducted to confirm the suitability of such a camera.
5. Simple studies have shown that analysis of guide camera images slightly outside and inside of focus just before beginning each science exposure will allow sufficiently frequent and accurate re-setting of telescope focus and top end alignment. This could be done with the top end hexapod providing the focus offsets but could be done quicker and more accurately by interchanging a set of plane parallel windows ahead of each camera.
6. Providing fiducials for calibration of the relationship between the guide sensor coordinates and the positioner coordinates should be straight-forward if it is accepted that the tolerance on the *predictability* of their relationship to the camera sensor coordinates need be no better than 2µm rms, rather than an absolute 1 µm.
7. Considerations of dark noise and seeing degradation have indicated that no cooling of the cameras will be needed.

Downloaded From: https://www.spiedigitallibrary.org/conference-proceedings-of-spie on 26 Jan 2021
Terms of Use: https://www.spiedigitallibrary.org/terms-of-use

REFERENCES

1. K.Szeto et al. “Mauna Kea Spectroscopic Explorer design development from feasibility concept to baseline design” Proc. SPIE 9906, 990691 (2016)
2. W. Saunders, P. Gillingham. “Optical designs for the Maunakea Spectroscopic Explorer Telescope” Proc. SPIE 9906, Ground-based and Airborne Telescopes VI
3. S.Smedly et al. “Sphinx: a massively multiplexed fiber positioned for MSE” Proc. SPIE 10702
4. Salmon, March 2019:”MSE guide star counts at the North Galactic Pole Ver.3.0” (file MSE guide star counts at the North Galactic Pole_ver.3.0.docx)
5. Salmon, Jan 2020: “MSE guide star counts in a crowded field updated Jan 2020” (file: MSE guide star counts in a crowded field 20200115.docx)
6. Salmon, October 2019: “A better look at MSE guide star centroid errors” (file: A better look at MSE guide star centroiding.docx)
7. https://www.teledynedalsa.com/en/products/imaging/cameras/genie-nano-1gige/
8. Gillingham March 2020: “MSE A&G CMOS camera sensor Effects of micro-lens ahead of photo-diode” (file: CMOS micro-lens effects.pptx)
9. Gillingham Dec. 2018: “MSE control of focus” (file: A&G_focus_control.pdf)
10. Gillingham Nov 2018 “MSE – detecting top end misalignment from out of focus images” (file: A&G_detecting_align_errors.pdf)
11. Beckers & Melnick, 1994 “Effects of heat sources in the telescope beam on astronomical image quality”, SPIE Vol 2199, pp 478-480.

Downloaded From: https://www.spiedigitallibrary.org/conference-proceedings-of-spie on 26 Jan 2021
Terms of Use: https://www.spiedigitallibrary.org/terms-of-use